

The Response of 6061-T6 Aluminum Alloy Tubes with Different Chop Depths under Cyclic Bending

Kuo-Long Lee^{1*}, Ruey-Terng Chern², Wen-Fung Pan³

¹ Department of Innovative Design and Entrepreneurship Management, Far East University

²⁻³ Department of Engineering Science, National Cheng Kung University

ABSTRACT

In this paper, the mechanical behavior and buckling failure of 6061-T6 aluminum alloy tubes with different chop depths subjected to cyclic bending were experimentally investigated. It can be seen that the moment-curvature relationship exhibits a steady loop from the first bending cycle. And, the chop depth has almost no influence on the moment-curvature relationship. However, the ovalization-curvature relationship exhibits an increasing and ratcheting manner with the number of the bending cycles. In addition, higher chop depth of a tube leads to a more severe unsymmetrical trend of the ovalization-curvature relationship. Furthermore, the 6061-T6 aluminum alloy tubes with five different chop depths were tested, five unparallel straight lines were found for the controlled curvature-number of cycles to produce buckling relationship in the log-log scale. Finally, the theoretical model proposed by Kyriakides and Shaw in 1987 was modified in this study for simulating the controlled curvature-number of cycles to produce buckling relationship. Through comparison with the experimental data, the theoretical model can properly simulate the experimental findings.

Key words: 6061-T6 Aluminum Alloy Tubes, Different Chop Depths, Cyclic Bending, Moment, Curvature, Ovalization, Buckling.

不同切痕深度 6061-T6 鋁合金圓管在循環彎曲負載下行為之研究

李國龍^{1*} 沈睿騰² 潘文峰³

¹ 遠東科技大學創新設計與創業管理系

²⁻³ 國立成功大學工程科學系

摘 要

本文係實驗研究不同切痕深度6061-T6鋁合金管在循環彎曲負載下的相關力學行為與皺曲損壞。根據實驗結果顯示，彎矩-曲度關係從第一圈開始便呈現一個穩定的迴圈，且切痕深度對彎矩-曲度關係幾乎沒有影響。至於橢圓化-曲度關係則隨著循環圈數的增加而呈現棘齒狀的成長，且切痕深度越大時，橢圓化-曲度關係就越不對稱，橢圓化量增加也就越大。此外，實驗測試有五種不同切痕深度6061-T6鋁合金管，而在雙對數座標的控制曲度-循環至皺曲圈數關係呈現五條不平行的直線。最後，本文修改Kyriakides and Shaw在1987年所提出的理論來描述控制曲度-循環至皺曲圈數的關係。在與實驗結果比較後發現，理論能夠合理描述實驗結果。

關鍵詞：6061-T6 鋁合金管、不同切痕深度、循環彎曲、彎矩、曲度、橢圓化、皺曲。

文稿收件日期 103. 10. 28；文稿修正後接受日期 104. 12. 17；*通訊作者

Manuscript received October 28, 2014；revised December 17, 2015；*Corresponding author.

I. INTRODUCTION

The bending of circular tubes leads to the ovalization of the tube's cross-section. The definition of ovalization is $\Delta D_o/D_o$ where D_o is the original outside diameter, D is the current diameter and ΔD_o is the change in outside diameter ($D_o - D$). Reverse bending and subsequent repeated cyclic bending may cause a gradual growth in ovalization. The increasing ovalization causes a progressive reduction in the bending rigidity of the tube. The tube will buckle when a critical magnitude of ovalization is reached. It is therefore of great importance to understand the response of circular tubes under cyclic bending in many industrial applications.

Since 1980, Kyriakides and his co-workers designed and constructed the tube cyclic bending machine and conducted a series of experimental and theoretical investigations. Shaw and Kyriakides [1] investigated the inelastic behavior of tubes subjected to cyclic bending. Kyriakides and Shaw [2] extended the analysis of tubes to the stability conditions under cyclic bending. Corona and Kyriakides [3] studied the degradation and buckling of tubes under cyclic bending and external pressure. Vaze and Corona [4] experimentally investigated the elastic-plastic degradation and collapse of steel tubes with square cross-sections under cyclic bending. Corona and Kyriakides [5] studied the asymmetric collapse modes of pipes under combined bending and pressure. Corona et al. [6] used a set of bending experiments to conduct on aluminum alloy tubes for investigating the yield anisotropy effects on the buckling. Limam et al. [7] studied the inelastic bending and collapse of tubes in present of the bending and internal pressure. Hallai and Kyriakides [8] experimentally studied the effect of Lüders bands on the bending of steel tubes. Limam et al. [9] investigated the collapse of dented tubes under combined bending and internal pressure.

In addition, other scholars have also published a number of related studies. Elchalakani et al. [10] experimentally conducted tests on the different diameter-to-thickness (D_o/t) ratios of grade C350 steel tubes under pure bending, and proposed two theoretical simulation models. Jiao and Zhao [11] tested the bending behavior of very high

strength (VHS) circular steel tubes, and proposed their plastic slenderness limit. Houliara and Karamanos [12] investigated the buckling and post-buckling of long pressurized elastic thin-walled tubes under in-phase bending. Elchalakani et al. [13] conducted the variable amplitude cyclic pure bending tests to determine fully ductile section slenderness limits for cold-formed CHS. Mathon and Liman [14] experimentally studied the collapse of thin cylindrical shell submitted to internal pressure and pure bending. Elchalakani and Zhao [15] investigated the concrete-filled cold-formed circular steel tubes subjected to variable amplitude cyclic pure bending. Fatemi et al. [16] discussed the parameters affecting the buckling and post-buckling behavior of high strength pipelines under bending. Suzuki et al. [17] researched the local buckling behavior of 48 high-strain line pipes under bending.

In 1998, Pan et al. [18] designed and set up a new measurement apparatus. It was used with the cyclic bending machine to study various kinds of tubes under different cyclic bending conditions. For instance, Pan and Fan [19] studied the effect of the prior curvature-rate at the preloading stage on the subsequent creep (moment is kept constant for a period of time) or relaxation (curvature is kept constant for a period of time) behavior, Pan and Her [20] investigated the response and stability of 304 stainless steel tubes subjected to cyclic bending with different curvature-rates, Lee et al. [21] studied the influence of the D_o/t ratio on the response and stability of circular tubes subjected to symmetrical cyclic bending, Lee et al. [22] experimentally explored the effect of the D_o/t ratio and curvature-rate on the response and stability of circular tubes subjected to cyclic bending, Chang et al. [23] studied the influence of the mean moment effect on circular thin-walled tubes under cyclic bending, Chang and Pan [24] discussed the buckling life estimation of circular tubes subjected to cyclic bending.

In practical industrial applications, tubes are under the hostile environment, so the material in the environment may corrode the tube surface and produce notches. The mechanical behavior and buckling failure of a notched tube differs from that of a tube with a smooth surface. In 2010, Lee et al. [25] studied the variation in ovalization of sharp-notched

circular tubes subjected to cyclic bending. Lee [26] investigated the mechanical behavior and buckling failure of sharp-notched circular tubes under cyclic bending. Lee et al. [27] experimentally discussed the viscoplastic response and collapse of sharp-notched circular tubes subjected to cyclic bending. Lee and Chang [28] investigated the response of sharp-notched 6061-T6 aluminum alloy tubes subjected to pure bending creep and relaxation.



Fig. 1. Picture of a tube with a circumferential sharp notch.

However, all investigations of the sharp notch were the circumferential sharp notch as shown in Fig. 1. If the sharp notch is a local sharp notch (Fig. 2), the response of a local sharp notch tube under cyclic bending should be different from that of a circumferential sharp notch tube under cyclic bending. Therefore, Lee et al. [29] investigated the response of local sharp-notched circular tubes with different notch depths subjected to cyclic bending. Lee et al. [30] studied the influence of the notch direction on the response of local sharp-notched circular tubes under cyclic bending.



Fig. 2. Picture of a tube with a local sharp notch.

It is known that the tubes may be damaged by a sharp object during the delivery, installation or use. Once a chop is on a tube

(Fig. 3), the response of the chopped tube under cyclic bending should be different from that of a smooth or other kind of notch tube under cyclic bending. Therefore, the response of 6061-T6 aluminum alloy tubes with different chop depths under cyclic bending was investigated in this paper.

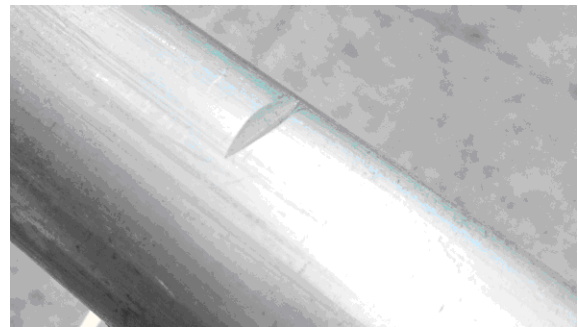


Fig. 3. Picture of a tube with a chop.

A four-point bending machine was used to conduct the chopped circular tubes under cyclic bending. A curvature-ovalization measurement apparatus (COMA) designed and reported previously by Pan et al. [18] was used to control the curvature. For chopped tubes, five different chop depths, 0.4, 0.8, 0.12, 1.6 and 2.0 mm, were considered in this study. The magnitude of the bending moment was measured by two load cells mounted in the bending device, and the magnitudes of the curvature and ovalization of the tube's cross-section were measured by COMA. In addition, the number of cycles to produce buckling was also recorded.

II. EXPERIMENT FACILITIES

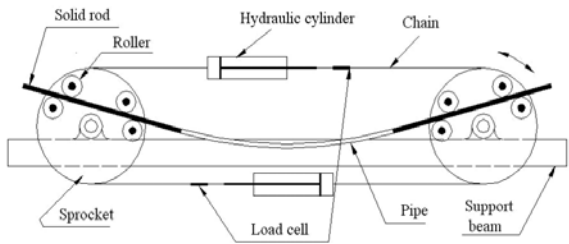
Bending Device

Fig. 4(a) shows a picture of the bending device and Fig. 4(b) is a schematic drawing of the bending device. It is designed as a four-point bending machine, capable of applying bending and reverse bending. The device consists of two rotating sprockets resting on two support beams. Heavy chains run around the sprockets and are connected to two hydraulic cylinders and load cells forming a closed loop. Each tube is tested and fitted with solid rod extension. The contact between the tube and the rollers is free to move along axial direction during bending. The load transfer to

the test specimen is in the form of a couple formed by concentrated loads from two of the rollers. Once either the top or bottom cylinder is contracted, the sprockets are rotated, and pure bending of the test specimen is achieved. Reverse bending can be achieved by reversing the direction of the flow in the hydraulic circuit. Detailed description of the bending device can be found in Shaw and Kyriakides [1] and Pan et al. [18].



(a)



(b)

Fig. 4. (a) A picture of the bending device and (b) a schematic drawing of the bending device.

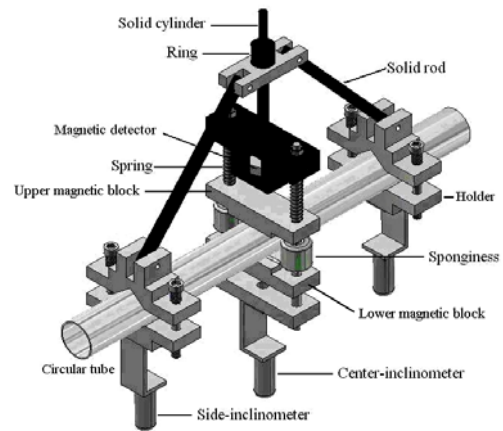
The two sprockets rest on two heavy support beams 1.25 m apart. This allows a maximum length of the test specimen to be 1 m. The bending capacity of the machine is 5300 N-m. Each tube is tested and fitted with a solid rod extension. The contact between the tube and the rollers is free to move along the axial direction during bending. The load transfer to the test specimen is a couple formed by concentrated loads from two of the rollers. The applied bending moment is directly proportional to the tension in the chains. Based on the signal from two load cells, the bending moment M exerted on the tube is calculated as

$$M = F R \quad (1)$$

where F is the force on the chain, which can be obtained from the pressure and area of the cylinder, and R is the radius of the sprocket.



(a)



(b)

Fig. 5. (a) A picture of the COMA and (b) a schematic drawing of the COMA.

Curvature-Ovalization Measurement Apparatus (COMA)

Fig. 5(a) shows a picture of the COMA and Fig. 5(b) shows a schematic drawing of the COMA. It is a lightweight instrument mounted close to the tube mid-span. There are three inclinometers in the COMA. Two inclinometers are fixed on two holders, which are denoted as side-inclinometers. These holders are fixed on the circular tube before the test begins. The distance between the two side-inclinometers is denoted as L_0 . Let us now consider that the circular tube is subjected to pure bending, as shown in Fig. 6. The angle changes detected by two side-inclinometers are denoted as θ_1 and θ_2 . From Fig. 3, the value of L_0 is determined as

$$L_0 = \rho (\theta_1 + \theta_2) \quad (2)$$

where ρ is the radius of the curvature. The curvature of the tube κ is

$$\kappa = 1 / \rho = (\theta_1 + \theta_2) / L_0 \quad (3)$$

In addition, a magnetic detector in the middle part of the COMA is used to measure the change in the outside diameter.

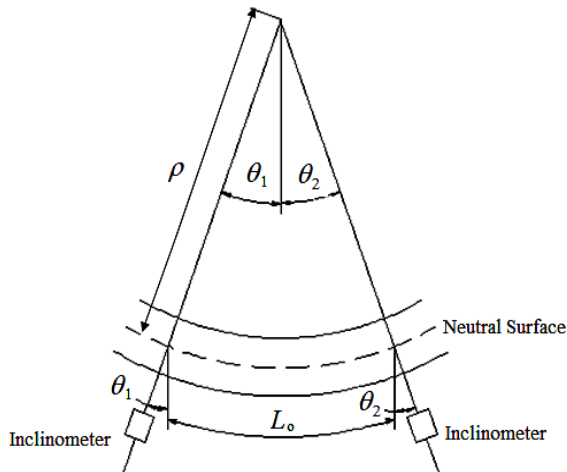


Fig. 6. Longitudinal deformation between two side-inclinometers under pure bending.

III. MATERIAL, SPECIMENS AND TEST PROCEDURES

Material

Circular tubes made of 6061-T6 aluminum alloy were used in this study. Table 1 shows its proportion of the chemical composition. The ultimate stress, 0.2% strain offset the yield stress and the percent elongation are 258 MPa, 166 MPa and 23%, respectively.

Table 1 Chemical composition of 6061-T6 aluminum alloy

Chemical Composition	Al	Mg	Si	Cu	Ti	Fe
Proportion (%)	97.40	0.916	0.733	0.293	0.268	0.256
Chemical Composition	Mn	Zn	Cr	Ni	Pb	Sn
Proportion (%)	0.132	0.0983	0.0682	0.0056	0.005	<0.001

Specimens

The raw smooth 6061-T6 aluminum alloy tubes had an outside diameter D_o of 35.0 mm and wall-thickness t of 3.0 mm. The raw tubes were machined on the outside surface to obtain the desired shape and depth of the chop. Fig. 7(a) shows a schematic drawing of the chopped

tube where the chop depth is denoted as a . In this study, five different chop depths were considered including 0.4, 0.8, 1.2, 1.6 and 2.0 mm, respectively. The chop root radius for all tested tubes was controlled to be less than 1/100 mm and all tested tubes were carefully examined before the test. Fig. 7(b) shows a picture of the tested 6061-T6 aluminum alloy tubes with different chop depths.

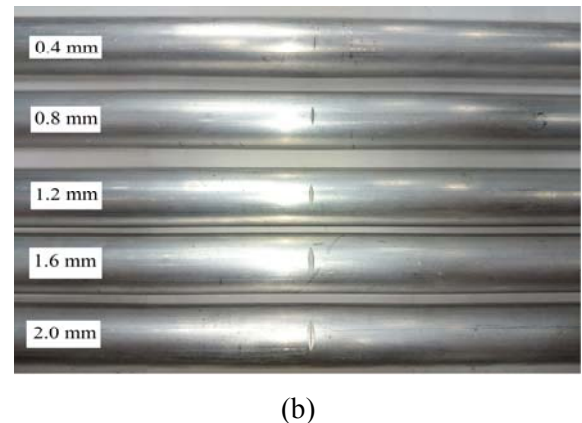
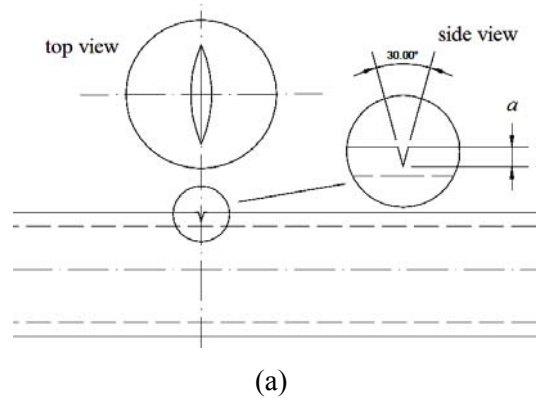


Fig. 7. (a) A schematic drawing of the chopped tube with a chop depth of a and (b) a picture of the tested 6061-T6 aluminum alloy tubes with different chop depths.

Test Procedures

The test involved a curvature-controlled cyclic bending. The curvature-rate of the cyclic bending test was $0.035 \text{ m}^{-1}\text{s}^{-1}$. The magnitude of the bending moment was measured by two load cells mounted in the bending device. The magnitudes of the curvature and ovalization of the tube cross-section were controlled and measured by the COMA.

IV. EXPERIMENTAL RESULTS, SIMULATED RESULTS AND DISCUSSION

Response of Chopped 6061-T6 Aluminum Alloy Tubes under Cyclic Bending

Fig. 8 shows the experimentally determined cyclic moment (M) - curvature (κ) for chopped 6061-T6 aluminum alloy tubes under cyclic bending with $a = 0.4$ mm. It can be seen that the tube exhibits a steady loop from the first cycle. Because the type of a chop is small and local, the chop depth has almost no influence on the M - κ curve. Therefore, the M - κ curves for different values of a are not shown in this paper. Lee [26] and Lee et al. [29] tested SUS304 stainless steel tubes with a circumferential sharp notch and a local sharp notch under cyclic bending, respectively, and discovered cyclic hardening of the M - κ curves. Similarly, the type of a local sharp notch is small and local, the notch depth has almost no influence on the M - κ curve [29]. As for the tube with a circumferential sharp notch, higher notch depth leads to a smaller wall-thickness, thus, the M - κ loops are different for different notch depth [26].

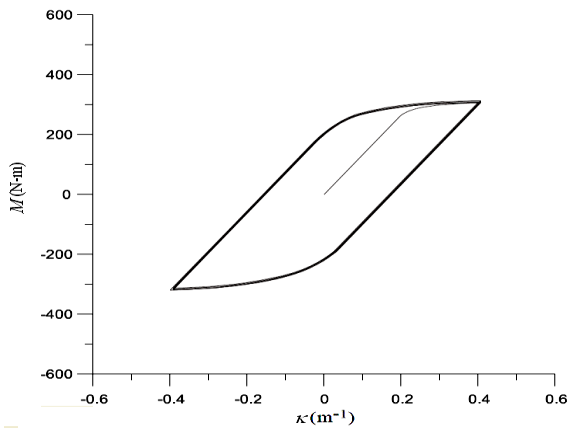
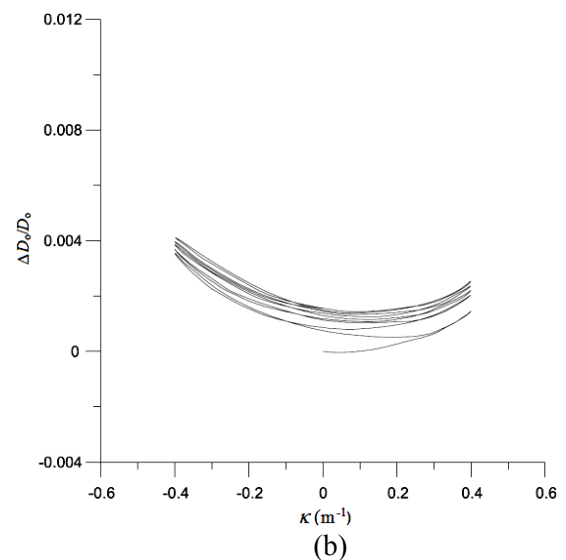
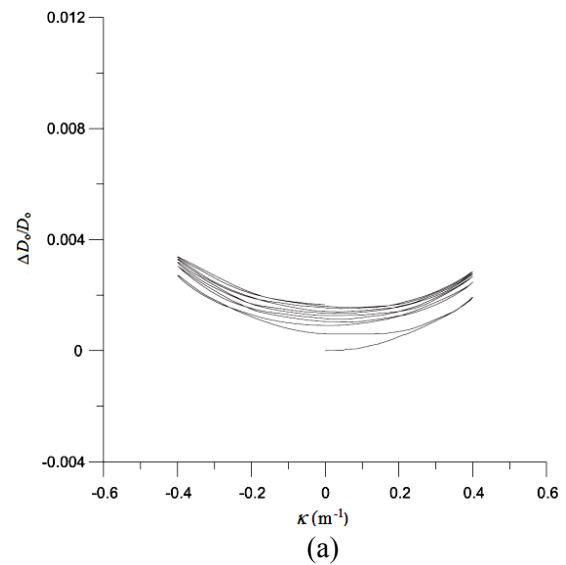


Fig. 8. Experimental moment (M) - curvature (κ) curves for 6061-T6 aluminum alloy tubes under cyclic bending with $a = 0.4$ mm.

Figs. 9(a)-(e) depict the experimentally determined cyclic ovalization ($\Delta D_o/D_o$) - curvature (κ) for 6061-T6 aluminum alloy tubes with $a = 0.4, 0.8, 1.2, 1.6$ and 2.0 mm, respectively. It can be seen that the ovalization increases in a ratcheting manner with the number of bending cycles. As the cyclic process continues, the ovalization keeps accumulating. Although the test is symmetrical cyclic bending (controlled cyclic curvature from $+0.4 \text{ m}^{-1}$ to

-0.4 m^{-1}), higher a of the chopped tube leads to a more severe unsymmetrical trend of the $\Delta D_o/D_o$ - κ curve. In addition, higher a of the chopped tube causes greater ovalization of the tube's cross-section. Although the increasing magnitudes of ovalization are different for SUS304 stainless steel tubes with a circumferential sharp notch [26], SUS304 stainless steel tubes a local sharp notch [29] or 6061-T6 aluminum alloy tubes with a chop under cyclic bending, but the aforementioned phenomena are similar.



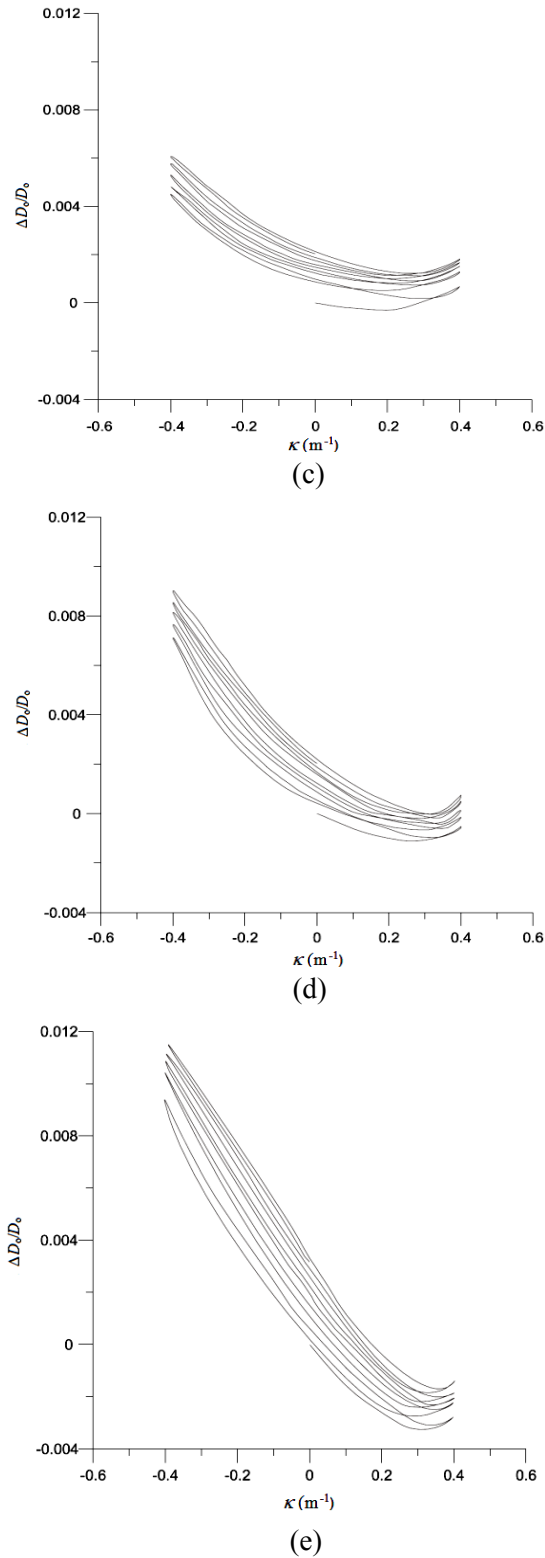


Fig. 9. Experimental ovalization ($\Delta D_0/D_0$) - curvature (κ) curves for 6061-T6 aluminum alloy tubes under cyclic bending with $a =$ (a) 0.4, (b) 0.8, (c) 1.2, (d) 1.6 and (e) 2.0 mm.

Buckling of Chopped 6061-T6 Aluminum Alloy Tubes under Cyclic Bending

Fig. 10 shows the experimental results of the controlled curvature (κ_c/κ_0) versus the number of cycles necessary to produce buckling (N_b) for 6061-T6 aluminum alloy tubes with $a = 0.4, 0.8, 1.2, 1.6$ and 2.0 mm. The quantity of κ_0 is used to normalize the κ_c which is defined as t/D_0^2 [2]. If we consider a given curvature, higher a leads to a lower value of N_b . This phenomenon can also be found from the tested data of SUS304 stainless steel tubes with a circumferential sharp notch [26] or a local sharp notch [29] under cyclic bending.

The results of Fig. 10 are plotted on a double logarithmic scale in Fig. 11 in dotted lines. The five straight dotted lines in this figure are least square fits of the data. These five straight dotted lines exhibit different slopes and intercepts. That is these five straight dotted lines are unparallel. This phenomenon is different from the experimental results obtained by Lee [26] and Lee et al. [29]. Although the κ_c-N_b curves plotted on a double logarithmic scale are all straight lines, but the straight lines are parallel to each other for SUS304 stainless steel tubes with a circumferential sharp notch and a local sharp notch under cyclic bending, respectively.

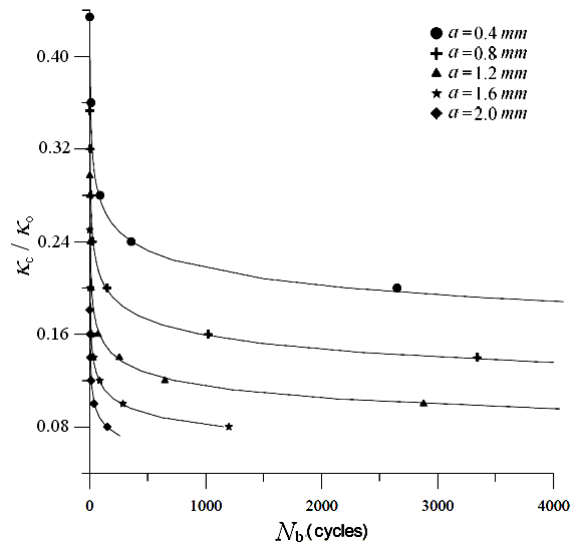


Fig. 10. Experimental controlled curvature (κ_c/κ_0) versus the number of cycles to produce buckling (N_b) for 6061-T6 aluminum alloy tubes with $a = 0.4, 0.8, 1.2, 1.6$ and 2.0 mm.

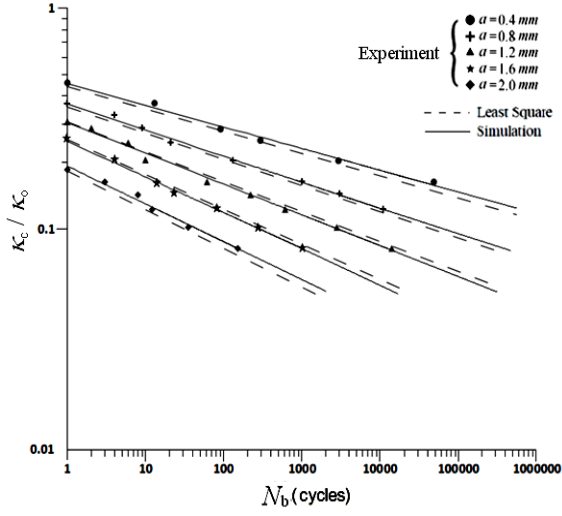


Fig. 11. Experimental and simulated controlled curvature (κ_c/κ_0) versus the number of cycles to produce buckling (N_b) for 6061-T6 aluminum alloy tubes with $a = 0.4, 0.8, 1.2, 1.6$ and 2.0 mm on a log-log scale.

Kyriakides and Shaw [2] have proposed a formulation of the relationship between κ_c/κ_0 and N_b for the material they tested as

$$\kappa_c/\kappa_0 = C (N_b)^{-\alpha} \quad (4)$$

or

$$\log \kappa_c/\kappa_0 = \log C - \alpha \log N_b \quad (5)$$

where C and α are the material parameters, which are related to the material properties and the D_o/t ratio. The material parameter C is the controlled curvature magnitude at $N_b = 1$, and α is the slope in the log-log plot. According to the experimental data, five quantities of C and α can be determined for $a = 0.4, 0.8, 1.2, 1.6$ and 2.0 mm in Table 2.

Table 2. Experimentally determined values of C and α .

a (mm)	0.4	0.8	1.2	1.6	2.0
C	0.443	0.367	0.303	0.250	0.186
α	0.102	0.116	0.137	0.157	0.165

According to the distributions of the relationship between $\ln C$ and a/t in Fig. 12 and the relationship between $\ln \alpha$ and a/t in Fig. 13, the following empirical formulations were proposed as

$$\ln C = c_1 (a/t) + c_2 \quad (6)$$

and

$$\ln \alpha = d_1 (a/t) + d_2 \quad (7)$$

where c_1, c_2, d_1 and d_2 are material parameters. The magnitudes of c_1, c_2, d_1 and d_2 can be determined to be $-1.571, -0.591, 0.0947$ and -2.395 , respectively. Fig. 11 also shows the simulated results of the controlled curvature (κ_c/κ_0) versus the number of cycles necessary to produce buckling (N_b) for 6061-T6 aluminum alloy tubes with $a = 0.4, 0.8, 1.2, 1.6$ and 2.0 mm on a log-log scale in solid lines. It can be seen that good agreement between these two results has been achieved.

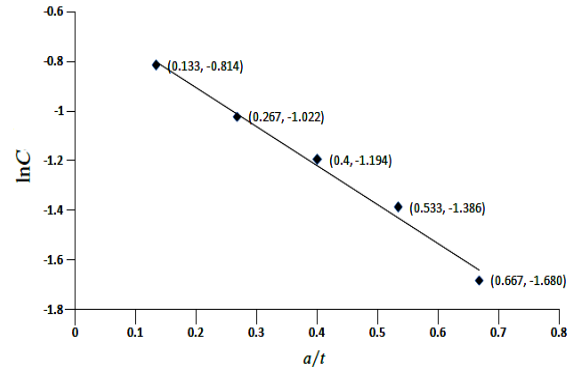


Fig. 12. Relationship between $\ln C$ and a/t .

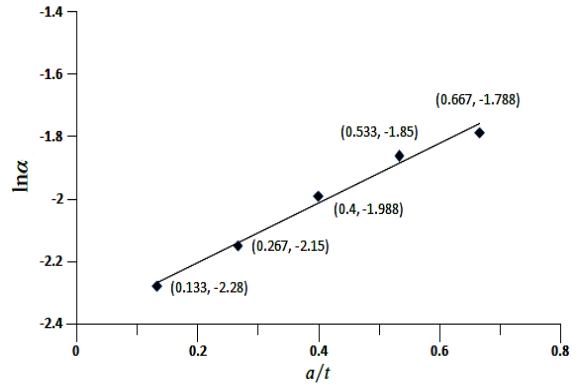


Fig. 13. Relationship between $\ln \alpha$ and a/t .

In practical application, the depth of the chop can not be precisely measured. In contrast, the length of the chop is more easily to get. Therefore, the relationship among chop length L_a, a and D_o is determined from the red right-triangle in Fig. 14 to be:

$$a = \frac{1}{2} D_o - \frac{1}{2} \sqrt{D_o^2 - L_a^2} \quad (8)$$

and

$$L_a = 2\sqrt{aD_o - a^2} \quad (9)$$

Thus, Eqs. (6) and (7) can also be expressed as a function of L_a to be:

$$\ln C = c_1 \left[\frac{1}{2} \frac{D_o}{t} - \frac{1}{2} \sqrt{\frac{D_o^2 - L_a^2}{t^2}} \right] + c_2 \quad (10)$$

and

$$\ln \alpha = d_1 \left[\frac{1}{2} \frac{D_o}{t} - \frac{1}{2} \sqrt{\frac{D_o^2 - L_a^2}{t^2}} \right] + d_2 \quad (11)$$

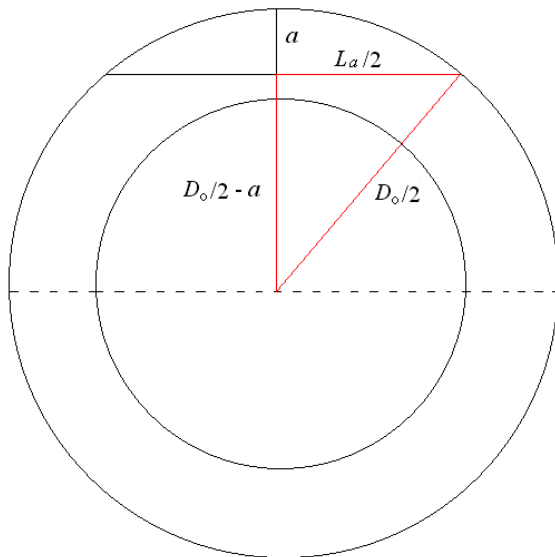


Fig. 14. Relationship among L_a , a and D_o .

V. CONCLUSIONS

The response of the chopped 6061-T6 aluminum alloy tubes with different chop depths subjected to cyclic bending were experimentally and theoretically investigated in this study. Based on the experimental and theoretical results, the following important conclusions can be drawn:

- (1) From the experimental $M-\kappa$ curves, the chopped 6061-T6 aluminum alloy tubes with any chop depth exhibit a steady loop from the first bending cycle. In addition, the shape and size of the $M-\kappa$ loop are very similar for any chop depth.
- (2) From the $\Delta D_o/D_o-\kappa$ curves, the ovalization of the tube cross-section increases in a ratcheting manner with the number of bending cycles.

Higher a leads to more unsymmetrical trend and greater ovalization of the tube's cross-section.

- (3) The formulation (Eq. (4)) proposed by Kyriakides and Shaw [2] was modified for simulating the relationship between κ/κ_0 and N_b for chopped 6061-T6 aluminum alloy tubes with $a = 0.4, 0.8, 1.2, 1.6$ and 2.0 mm under cyclic bending. The formulation of the parameters C and α were proposed in Eqs. (6) and (7), respectively. It can be seen that the simulation by Eqs. (4), (6) and (7) is in good agreement with the experimental result as shown in Fig. 11.

V. REFERENCES

- [1] Shaw, P. K. and Kyriakides, S., "Inelastic Analysis of Thin-walled Tubes under Cyclic Bending," *Int. J. Solids Struct.*, Vol. 21, No. 11, pp. 1073-1110, 1985.
- [2] Kyriakides, S. and Shaw, P. K., "Inelastic Buckling of Tubes under Cyclic Loads," *ASME J. Pre. Ves. Tech.*, Vol. 109, No. 2, pp. 169-178, 1987.
- [3] Corona, E. and Kyriakides, S., "An Experimental Investigation of the Degradation and Buckling of Circular Tubes under Cyclic Bending and External Pressure," *Thin-Walled Struct.*, Vol. 12, Is. 3, pp. 229-263, 1991.
- [4] Vaze, S. and Corona, E., "Degradation and Collapse of Square Tubes under Cyclic Bending," *Thin-Walled Struct.*, Vol. 31, No. 4, pp. 325-341, 1998.
- [5] Corona, E. and Kyriakides, S., "Asymmetric Collapse Modes of Pipes under Combined Bending and Pressure," *J. Eng. Mech.*, Vol. 126, No. 12, pp. 1232-1239, 2000.
- [6] Corona, E., Lee, L. H. and Kyriakides, S., "Yield Anisotropic Effects on Buckling of Circular Tubes under Bending," *Int. J. Solids Struct.*, Vol. 43, No. 22, pp. 7099-7118, 2006.
- [7] Limam, A., Lee, L. H., Corona, E. and Kyriakides, S., "Inelastic Wrinkling and Collapse of Tubes under Combined Bending and Internal Pressure," *Int. J. Mech. Sci.*, Vol. 52, Is. 5, pp. 637-647, 2010.

- [8] Hallai, J. F. and Kyriakides, S., "On the Effect of Lüders Bands on the Bending of Steel Tubes," *Int. J. Solids Struct.*, Vol. 48, Is. 24, pp. 3275-3284, 2011.
- [9] Limam, A., Lee, L. H. and Kyriakides, S., "On the Collapse of Dented Tubes under Combined Bending and Internal Pressure," *Int. J. Mech. Sci.*, Vol. 55, Is. 1, pp. 1-12, 2012.
- [10] Elchalakani, M., Zhao, X. L. and Grzebieta, R. H., "Plastic Mechanism Analysis of Circular Tubes under Pure Bending," *Int. J. Mech. Sci.*, Vol. 44, No. 6, pp. 1117-1143, 2002.
- [11] Jiao, H. and Zhao, X. L., "Section Slenderness Limits of Very High Strength Circular Steel Tubes in Bending," *Thin-Walled Struct.*, Vol. 42, No. 9, pp. 1257-1271, 2004.
- [12] Houliara, S. and Karamanos, S. A., "Buckling and Post-buckling of Long Pressurized Elastic Thin-walled Tubes under In-plane Bending," *Int. J. Nonlinear Mech.*, Vol. 41, No. 4, pp. 491-511, 2006.
- [13] Elchalakani, M., Zhao, X. L. and Grzebieta, R. H., "Variable Amplitude Cyclic Pure Bending Tests to Determine Fully Ductile Section Slenderness Limits for Cold-formed CHS," *Eng. Struct.*, Vol. 28, Is. 9, pp. 1223-1235, 2006.
- [14] Mathon, C. and Liman, A., "Experimental Collapse of Thin Cylindrical Shells Submitted to Internal Pressure and Pure Bending," *Thin-Walled Struct.*, Vol. 44, No. 1, pp. 39-50, 2006.
- [15] Elchalakani, M. and Zhao, X. L., "Concrete-filled Cold-formed Circular Steel Tubes Subjected to Variable Amplitude Cyclic Pure Bending," *Eng. Struct.*, Vol. 30, No. 2, pp. 287-299, 2008.
- [16] Fatemi, A., Kenny, S., Sen, M., Zhou, J., Tahern, F. and Paulin, M., "Parameters Affecting Buckling and Post-buckling Behavior of High Strength Pipelines," *Proceeding of the 28th International Conference on Ocean, Offshore Mechanics and Arctic Engineering*, Hawaii, U.S.A., 2009.
- [17] Suzuki, N., Tajika, H., Igi, S., Okatsu, M., Kondo, J. and Arakawa, T., "Local Buckling Behavior of 48 High-strain Line Pipes," *Proceeding of the eighth International Pipeline Conference*, Alberta, Canada, 2010.
- [18] Pan, W. F., Wang, T. R. and Hsu, C. M., "A Curvature-Ovalization Measurement Apparatus for Circular Tubes under Cyclic Bending," *Exp. Mech.*, Vol. 38, No. 2, pp. 99-102, 1998.
- [19] Pan, W. F. and Fan, C. H., "An Experimental Study on the Effect of Curvature-rate at Preloading Stage on Subsequent Creep or Relaxation of Thin-walled Tubes under Pure Bending," *JSME Int. J., Ser. A*, Vol. 41, No. 4, pp. 525-531, 1998.
- [20] Pan, W. F. and Her, Y. S., "Viscoplastic Collapse of Thin-walled Tubes under Cyclic Bending," *ASME J. Eng. Mat. Tech.*, Vol. 120, No. 4, pp. 287-290, 1998.
- [21] Lee, K. L., Pan, W. F. and Kuo, J. N., "The Influence of the Diameter-to-thickness Ratio on the Stability of Circular Tubes under Cyclic Bending," *Int. J. Solids Struct.*, Vol. 38, No. 14, pp. 2401-2413, 2001.
- [22] Lee, K. L., Pan, W. F. and Hsu, C. M., "Experimental and Theoretical Evaluations of the Effect between Diameter-to-thickness Ratio and Curvature-rate on the Stability of Circular Tubes under Cyclic Bending," *JSME Int. J., Ser. A*, Vol. 47, No. 2, pp. 212-222, 2004.
- [23] Chang, K. H., Pan, W. F. and Lee, K. L., "Mean Moment Effect of Thin-walled Tubes under Cyclic Bending," *Struct. Eng. Mech.*, Vol. 28, No. 5, pp. 495-514, 2008.
- [24] Chang, K. H. and Pan, W. F., "Buckling Life Estimation of Circular Tubes under Cyclic Bending," *Int. J. Solids Struct.*, Vol. 46, No. 2, pp. 254-270, 2009.
- [25] Lee, K. L., Hung, C. Y. and Pan, W. F., "Variation of Ovalization for Sharp-notched Circular Tubes under Cyclic Bending," *J. Mech.*, Vol. 26, No. 3, pp. 403-411, 2010.
- [26] Lee, K. L., "Mechanical Behavior and Buckling Failure of Sharp-notched Circular Tubes under Cyclic Bending," *Struct. Eng. Mech.*, Vol. 34, No. 3, pp. 367-376, 2010.
- [27] Lee, K. L., Hsu, C. M. and Pan, W. F.,

- “Viscoplastic Collapse of Sharp-notched Circular Tubes under Cyclic Bending,” *Acta Mech. Solida Sinica*, Vol. 22, No. 6, pp. 629-641, 2013.
- [28] Lee, K. L. and Chang, K. H., “The Mechanical Behavior and Buckling Failure of Sharp-notched 6061-T6 Aluminum Alloy Tubes under Pure Bending Creep and Relaxation,” *J. Chung Cheng Inst. Tech.*, Vol. 43, No. 2, pp. 52-60, 2014.
- [29] Lee, K. L. Meng, C. H. and Pan, W. F., “The Influence of Notch Depth on the Response of Local Sharp-notched Circular Tubes under Cyclic Bending,” *J. Appl. Math. Phys.*, Vol. 2, No. 6, pp. 335-341, 2014.
- [30] Lee, K. L. Chang, K. H. and Pan, W. F., “Experimental and Theoretical Evaluations of the Effect of Notch Directions on the Stability of Local Sharp-notched Circular Tubes under Cyclic Bending,” submitted to *Int. J. Appl. Mech.*, 2015.